Available online at www.sciencedirect.com
SCIENCE DIRECT®
Journal of Computational Physics 201 (2004) 148–171
JOURNAL OF COMPUTATIONAL PHYSICS
www.elsevier.com/locate/jcp

Non-Monte Carlo formulations and computational techniques for the stochastic non-linear Schrödinger equation ☆

Alper Demir *

Department of Electrical and Electronics Engineering, Koc University, Rumeli Feneri Yolu, 34450 Sariyer-Istanbul, Turkey

Received 24 October 2003; received in revised form 12 May 2004; accepted 13 May 2004
Available online 24 June 2004

Abstract

Stochastic ordinary and partial differential equations (SOPDEs) in various forms arise and are successfully utilized in the modeling of a variety of physical and engineered systems such as telecommunication systems, electronic circuits, cosmological systems, financial systems, meteorological and climate systems. While the theory of stochastic partial and especially ordinary differential equations is more or less well understood, there has been much less work on practical formulations and computational approaches to solving these equations. In this paper, we concentrate on the stochastic non-linear Schrödinger equation (SNLSE) that arises in the analysis of wave propagation phenomena, mainly motivated by its predominant role as a modeling tool in the design of optically amplified long distance fiber telecommunication systems. We present novel formulations and computational methods for the stochastic characterization of the solution of the SNLSE. Our formulations and techniques are not aimed at computing individual realizations, i.e., sample paths, for the solution of the SNLSE á la Monte Carlo. Instead, starting with the SNLSE, we derive new systems of differential equations and develop associated computational techniques. The numerical solutions of these new equations directly produce the ensemble-averaged stochastic characterization desired for the solution of the SNLSE, in a non-Monte Carlo manner without having to compute many realizations needed for ensemble-averaging.

Keywords: Stochastic partial differential equations; Stochastic non-linear Schrödinger equation; Noise analysis; Optical fiber communications; Linearly implicit integration methods; Lyapunov matrix equation; Non-stationary noise; Spectral methods

☆ This work was sponsored by the Turkish Academy of Sciences GEBIP program.
* Tel.: +90-212-338-1706; fax: +90-212-338-1548.
E-mail address: aldemir@ku.edu.tr.
URL: http://home.ku.edu.tr/~aldemir.

0021-9991/$ - see front matter
doi:10.1016/j.jcp.2004.05.009

1. Introduction

Stochastic models in the form of stochastic ordinary and partial differential equations (SOPDEs) are used for the representation and analysis of various kinds of situations and systems. For example, random variables and stochastic processes are used to represent fluctuating external forces on the system under consideration. In other cases, they are used to model system parameters that fluctuate with time or take random values for different realizations of the system. SOPDEs are also utilized to significantly reduce the number of equations and variables in a dynamical system model by exploiting multiscale behavior and representing rapidly varying "modes" as stochastic forcing [1]. SOPDEs naturally arise in the modeling of a variety of physical and engineered systems such as telecommunication systems [2], electronic circuits [3], cosmological systems [4], financial systems [5], meteorological and climate systems [1].

The theory of SOPDEs is quite well developed [6–9]. However, there is much less work in the literature on practical computational approaches to solving these equations. Moreover, most of the work on numerical techniques for SPODEs has been concentrated on stochastic differential (not partial) equations, and they are directed at computing individual realizations or sample paths for the solution [10,1]. In most practical applications, a compact ensemble-averaged stochastic characterization of the solution is needed. With approaches that compute individual realizations for the solution, such stochastic characterizations can be obtained via the Monte Carlo method, by generating many sample paths for the solution followed by ensemble-averaging for quantities of interest. Since a large number of sample paths are typically required for meaningful statistics, Monte Carlo approaches are usually inefficient [3]. Moreover, they may also run into accuracy problems [3]. To address these problems with the Monte Carlo approach, Fokker–Planck equation based approaches have been proposed [1,3,11,12]. The Fokker–Planck equation is a partial differential equation for the multi-dimensional time-varying probability density for the variables of the original SOPDE. Numerically solving for the density of a multivariate system is often prohibitively expensive due to mainly the very large size of the state space that must be sampled [1,3]. Fokker–Planck equation based approaches have been successful only in cases where the number of variables (including the additional variables that may have been generated using the method of lines for SPDEs) in the SOPDE is not more than a few [1,11,12]. The solution of the Fokker–Planck equation produces the full time-varying multivariate probability density, which can be used to compute all kinds of compact stochastic characterizations required by the application. However, in most applications, the full probability density is not really required. Instead, only up to second-order probabilistic characterizations, i.e., time-varying means and variances of, and covariances among, the variables are more than sufficient. This can be inferred by considering that even nonlinear systems behave approximately linearly with small fluctuating noisy excitations, and that most noise sources that arise in both physical and engineered systems are approximately Gaussian due to the Central Limit Theorem. For Gaussian random variables, means, variances and correlations fully specify the multivariate density. Linear transformations of Gaussian random variables and stochastic processes are also Gaussian. Thus, the compact probabilistic characterization required by the application can be computed using only these first- and second-order moments of the probability density [3].

In this paper, we concentrate on the stochastic non-linear Schrödinger equation (SNLSE) that arises in the analysis of wave propagation phenomena in various situations and systems. We are mainly motivated by the predominant role of the SNLSE as a modeling tool in the design of optically amplified long distance fiber telecommunication systems [2]. We use optical fiber communication systems as a case study to demonstrate the practical applicability and usefulness of our work. In Section 2, we present a short overview of optical fiber communication systems and the challenges that faces one from a modeling, analysis and design perspective. We also discuss the importance of the SNLSE in this field as the governing

equation for signal and noise propagation in optical fibers. We provide Section 2 for the reader who is interested in learning about optical fiber communication systems, and for a discussion of the background and terminology needed for a better appreciation of the computational results that will be presented in Section 5. The reader who is interested only in the formulations and the computational techniques for the SNLSE can skip Section 2 without loss of continuity. We believe that the usefulness of the work presented in the paper is by no means restricted to the analysis of optical fiber communication systems, and that it will find applications in the analysis of other stochastic wave propagation phenomena, and that it is a novel and worthwhile contribution in the general setting of computational techniques for stochastic partial differential equations.

We first present novel formulations and computational methods for the stochastic characterization of the solution of the SNLSE. Unlike almost all previous approaches, our formulations and techniques are not aimed at computing individual realizations, i.e., sample paths, for the solution of the SNLSE á la Monte Carlo. Instead, in Section 3, starting with the SNLSE, we formulate new systems of differential equations for the second-order moments, i.e., time-varying means, variances, correlation functions, and spectral densities for the solution of the SNLSE.

The numerical solutions of these new equations directly produce the ensemble-averaged stochastic characterization desired for the solution of the SNLSE, in a non-Monte Carlo manner without having to compute many realizations needed for ensemble-averaging. Our derivations are based on *linear*(*ized*) {*time,space*}*-varying, non-stationary* formulations. This approach is similar, in spirit, to the linear(ized), time-varying formulations for noise analysis in analog/RF electronic circuits, where the governing equations are systems of SODEs generated by Kirchoff's voltage and current laws [3].

Then, we develop computational techniques for the solution of these newly derived equations for the second-order stochastic characterization of the solution of the original SNLSE. In doing so, we utilize *linearly* (*diagonally*) *implicit multistep* (not to be confused with implicit linear multistep) integration methods. Linearly implicit multistep integration schemes were originally proposed for solving stiff non-linear PDEs [13,14]. In this work, we use the idea behind the linearly implicit schemes in a different context, for solving purely linear systems of differential equations that we derive for the second-order stochastic characterization discussed above. In Sections 4.2 and 4.3, we explain how we generalize the idea behind the linearly implicit schemes for our setting, and how we separate these purely linear sets of equations into stiff and non-stiff parts.

The contributions of this work can be summarized as follows:

- Two novel, non-Monte Carlo formulations for solving the stochastic non-linear Schrödinger equation: Section 3.
  - Covariance matrix based formulation: Section 3.2.
  - Frequency-decomposed formulation: Section 3.3.
- Novel, non-Monte Carlo, efficient and accurate computational techniques (that incorporate linearly implicit integration schemes) for the solution of the newly derived equations to produce practical compact ensemble-averaged probabilistic characterizations directly usable in applications. The computational techniques described in Section 4 feature.
  - Efficient numerical method for the solution of Lyapunov matrix equations with structured coefficient matrices: Section 4.2.
  - Efficient computation of the frequency dependence of spectral densities either using a parallelizable scheme or in approximate (Padé approximation) analytical (rational) form: Section 4.3.
- Practical application of the formulations and the computational techniques developed in the paper to the investigation of signal–noise mixing due to the optical fiber non-linearities in fiber-optic telecommunication systems and generation of design guidelines: Section 2 and Section 5.

2. Optical fiber communication systems and SNLSE

The optical fiber transmission links form the backbone of the communications infrastructure. Almost all of voice and data (internet) traffic is routed through terrestrial and submarine optical fiber links, connecting the world together. Invention of the optical amplifiers (OAs) and wavelength-division multiplexing (WDM) technology enabled very high capacity optical fiber communication links that run for thousands of kilometers without any electronic repeaters, but at the same time brought many design challenges.

In WDM optical fiber communications, information bits are used to modulate the (light) carriers at many wavelengths (colors), which are then transmitted in a single strand of fiber. The signal levels deteriorate during transmission due to the loss of the optical fiber, which need to be restored by OAs for reliable detection. OAs have very wide bandwidths, e.g., 4 THz, they can amplify many wavelength carriers (data channels) at once. As electronic amplifiers do, OAs add noise (∼white and stationary) to the signal they amplify. A long-haul optical fiber communication link may be several thousands of kilometers long, and it may have tens of optical amplification sites placed at regular intervals (∼80 km) along the link, as shown in Fig. 1. The information signals in a number of WDM channels and the noise added by the OAs travel together in the optical fiber and impinge on the electronic receiver. The optical fiber is a lossy, dispersive, and *non-linear* transmission medium. Due to the non-linearity of the fiber, the information signals at different wavelengths and noise added by the OAs mix with each other as they propagate together along the fiber. The propagation of the signals and noise in an optical fiber is governed by a *non-linear* partial differential equation (PDE), the so-called generalized non-linear Schrödinger equation (NLSE), which can be derived directly from Maxwell's equations that govern the propagation of light waves in a dielectric waveguide, i.e., the optical fiber.

In the design of an optical fiber communication link, the prediction of the deterioration the information signals experience due to the non-linearity of the optical fiber and the optical noise generated by the OAs is essential. The formulations and the computational techniques we develop in this paper can be used for the analysis of the mixing of the information signals with noise, as opposed to the mixing of the information signals with each other, due to the fiber non-linearity. We use this problem as a case study to demonstrate the practical applicability and usefulness of our techniques.

The mixing of the information signals with each other is also of great importance in systems design. We touch upon this phenomenon on several occasions in the paper, but a detailed treatment of signal–signal mixing analysis is beyond the scope of this work. There has been considerable effort and tremendous progress made on this problem in the literature. However, the need for more efficient, *semi-analytical* analysis techniques is still there.

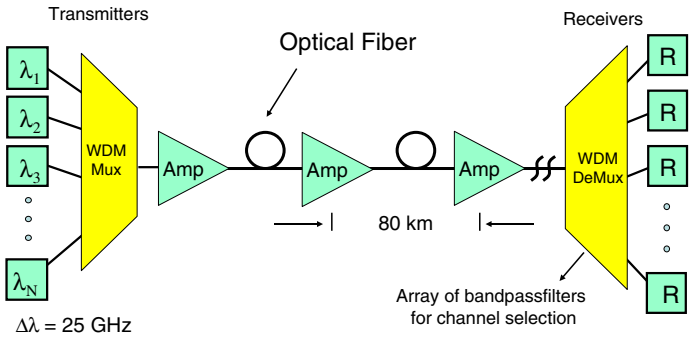

Fig. 1. WDM optical fiber communication link.

Commonly, the prediction of noise–signal mixing is performed with a *Monte Carlo* type propagation simulation, where the information signals and randomly generated optical noise are simulated together in a numerical solution of the NLSE. This kind of simulation is inefficient, because one needs to repeat the simulation for sufficiently many sample paths of the noise process. It also is incapable of providing systems design intuition. In a Monte Carlo type simulation, one simulates signal–signal and signal–noise mixing together, which hides the separate and quite different performance degradation mechanisms due to these mixing processes. The "separated" analysis of these mechanisms, in fact, provides valuable systems design intuition, as we will demonstrate in this paper.

There has also been analytical approaches to the noise–signal mixing analysis problem in optical fiber propagation, and considerable progress has been made. It was first investigated in 1990 by Gordon and Mollenauer [15]. In their original treatment, they considered a system with a *single unmodulated* carrier [1], and *ignored dispersion* in the fiber. The dispersion in the fiber is of paramount importance in the analysis of signal–noise mixing. Kikuchi [16] included dispersion in his analysis, but it was also restricted to a single unmodulated carrier. Poggiolini and Benedetto et. al. [17] considered a *multi-wavelength* system with a comb of *unmodulated* carriers [2] and took dispersion into account in their innovative analytical approach.

In this paper, we consider the most general case, a *multi-wavelength* system with *modulated carriers* [3] with dispersion included. The treatment of this most general case requires the concepts of *non-stationarity* and *frequency correlation* for stochastic processes, i.e., noise signals, which we will discuss later. In Section 3, we describe novel formulations for the analysis of the interplay, i.e., mixing, between the information signals, i.e., modulated light carriers, and the optical noise due to the fiber non-linearity. As with many other non-linear and non-stationary stochastic problems, the problem in hand is conceptually challenging and computationally complex. We try to alleviate these difficulties through the use of semi-analytical formulations and sophisticated numerical techniques for the computational problem. In this context, "semi-analytical" is used to mean that, even though the formulation itself is fully analytical, it does not yield to a closed-form solution, and still requires the numerical solution of (partial) differential equations. However, the equations that need to be solved are different, and involve different variables, compared with the ones solved with the *brute-force* Monte Carlo simulation approach. In particular, we use *linear*(*ized*) {*time,space*}*-varying, non-stationary* formulations. A linearization formulation was also used by Poggiolini et al. [17].

We describe, in Section 4, the numerical methods built on top of our formulations discussed above and their practical implementation for optical fiber communication link analysis. Then, in Section 5, we present results generated by the proposed and implemented techniques in the investigation of signal–noise mixing due to the optical fiber non-linearities. We discuss the use of the generated results in determining the performance of communication links, and discuss system design implications.

[1] An unmodulated carrier signal, in mathematical terms, has a spectrum with a single δ-function situated at the frequency of the monochromatic light generated by the laser. Hence, in time domain it is expressed as $\exp(\mathrm{j}\omega_c t)$, where $\mathrm{j} = \sqrt{-1}$ and ω_c is the frequency of the monochromatic light generated by the laser.

[2] A signal composed of a comb of unmodulated carriers, in mathematical terms, has a spectrum with a number of δ-functions situated at the frequencies of the light generated by multiple lasers. These δ-functions are typically equally spaced in frequency. Hence, in time domain we have $\exp(\mathrm{j}\omega_{c1} t) + \cdots + \exp(\mathrm{j}\omega_{cN} t)$ where ω_{c1} through ω_{cN} are the frequencies of the light generated by the multiple lasers.

[3] A modulated carrier signal can be expressed in mathematical terms as $m(t)\exp(\mathrm{j}\omega_c t)$, where $\mathrm{j} = \sqrt{-1}$, ω_c is the frequency of the monochromatic light generated by the laser, and $m(t)$ is the modulating information signal with a series of pulses encoding the 0s and 1s that need to transmitted. The spectrum of a modulated carrier is obviously not a δ-function, but occupies a certain band of frequencies around ω_c and has a certain functional form determined by the shapes, widths and the repetition rates of the pulses in the modulating function $m(t)$.

3. Non-Monte Carlo formulations for the solution of the stochastic NLSE

The non-linear Schrödinger equation that governs the evolution of the complex envelope $U(z,t)$ for the electric field of the propagating wave is given below

$$\frac{\partial U(z,t)}{\partial z} = -\frac{1}{2}\alpha U(z,t) - \mathrm{j}\frac{1}{2}\beta_2 \frac{\partial^2 U(z,t)}{\partial t^2} + \frac{1}{6}\beta_3 \frac{\partial^3 U(z,t)}{\partial t^3} + \mathrm{j}\gamma |U(z,t)|^2 U(z,t), \tag{1}$$

where t is time, z is the position along the propagation direction, α models the loss of the transmission medium (assumed frequency/wavelength independent here), the terms with β_2 and β_3 model second- and third-order dispersion (the effect of which is equivalent to an all-pass linear filter with phase distortion), the term with γ models the non-linearity of the transmission medium, and finally $\mathrm{j} = \sqrt{-1}$. First-order dispersion β_1 has been factored out through a change of the position variable z, since it amounts to a pure time delay, without any phase distortion. [4]

Next, we derive a linear PDE for perturbation/noise analysis, and then in Section 3.2, we describe a covariance matrix formulation for stochastic perturbation/noise characterization. This formulation directly produces the compact ensemble-averaged second-order probabilistic characterization needed. [5] In Section 3.3, we develop a frequency-decomposed formulation for perturbation/noise analysis. This alternative formulation has some benefits, its implementation can be parallelized for efficiency, and we further develop it into a reduced-order-modeling formalism. [6]

3.1. Derivation of linear PDE for perturbation analysis

Let $A(z,t)$ be the solution of (1) without any noise in the system. Hence $A(z,t)$ satisfies (1). We describe the numerical computation of $A(z,t)$ in Section 4. $A(z=0,t)$ is the initial condition. [7]

We now consider the system *with* noise and perform the following three operations in sequence:

1. substitute $U(z,t) = A(z,t) + a(z,t)$ in (1) where $a(z,t)$ is a perturbation to $A(z,t)$;
2. subtract (1), with $U(t,z)$ replaced by $A(z,t)$, from the result of the first step above;
3. for linear(ized) noise analysis, ignore all terms, in the result of the second step above, that are not linear in $a(z,t)$, justified by the fact that $a(z,t)$ is much "smaller" than $A(z,t)$.

and obtain

$$\frac{\partial a(z,t)}{\partial z} = -\frac{1}{2}\alpha a(z,t) - \mathrm{j}\frac{1}{2}\beta_2 \frac{\partial^2 a(z,t)}{\partial t^2} + \frac{1}{6}\beta_3 \frac{\partial^3 a(z,t)}{\partial t^3} + 2\mathrm{j}\gamma |A(z,t)|^2 a(z,t) + \mathrm{j}\gamma A(z,t)^2 a(z,t)^{\star}, \tag{2}$$

where $\star$ denotes "complex-conjugate". In (2), $a(z,t)$ is a complex-valued scalar function of z and t. We decompose $a(z,t)$ into its real (in-phase) and imaginary (quadrature) components

[4] Values of the parameters for loss, dispersion and non-linearity for various kinds of optical fibers are available. (1) can be derived directly from Maxwell's equations [18]. $U(z,t)$ is the *complex envelope* for the electric field. The *very* high frequency ($\sim$200 THz) lightwave carrier, as well as the transverse, i.e., $x-y$, electric field profile, have been factored out of (1) through some verified approximations [18]. $U(z,t)$ and (1) are normalized in such a way that $|U(z,t)|^2$ is the instantaneous optical power.

[5] The covariance matrix formulation produces a noise characterization which can be directly used in a communication system bit-error-rate (BER) performance evaluation.

[6] The frequency-decomposed formulation produces a noise characterization which can not be directly used in system BER performance evaluation. However, the proper noise characterization needed for BER evaluation can be easily computed from the frequency-decomposed noise characterization, which will be explained in Section 3.3.

[7] $A(z=0,t)$ is the signal launched into the fiber. Note here that we do *not* place a restriction on the launched signal $A(0,t)$. Authors in [17] assume that $A(0,t)$ is a *comb* of continuous-wave (CW), i.e., unmodulated, optical carriers. Moreover, with their formulation, they also ignore (four-wave) mixing among the carriers themselves.

$$a(z,t) = a_r(z,t) + \mathrm{j}a_i(z,t), \quad A(z,t) = A_r(z,t) + \mathrm{j}A_i(z,t). \tag{3}$$

With (3), (2) becomes

$$\begin{aligned}\frac{\mathrm{d}}{\mathrm{d}z}\begin{bmatrix} a_r(z,t) \\ a_i(z,t)\end{bmatrix} &= -\frac{1}{2}\alpha\begin{bmatrix} a_r(z,t) \\ a_i(z,t)\end{bmatrix} + \frac{1}{2}\beta_2\begin{bmatrix} 0 & \frac{\partial^2}{\partial t^2} \\ -\frac{\partial^2}{\partial t^2} & 0\end{bmatrix}\begin{bmatrix} a_r(z,t) \\ a_i(z,t)\end{bmatrix} + \frac{1}{6}\beta_3\begin{bmatrix} \frac{\partial^3}{\partial t^3} & 0 \\ 0 & \frac{\partial^3}{\partial t^3}\end{bmatrix}\begin{bmatrix} a_r(z,t) \\ a_i(z,t)\end{bmatrix} \\ &\quad + \gamma\begin{bmatrix} -2A_r(z,t)A_i(z,t) & -A_r(z,t)^2 - 3A_i(z,t)^2 \\ 3A_r(z,t)^2 + A_i(z,t)^2 & 2A_r(z,t)A_i(z,t)\end{bmatrix}\begin{bmatrix} a_r(z,t) \\ a_i(z,t)\end{bmatrix}.\end{aligned} \tag{4}$$

In the linear(ized) PDE (4) above, $A(z,t)$ is the deterministic signal, and $a(z,t)$ is the stochastic perturbation due to noise.

With the linearization performed above, we have effectively decomposed the solution of the SNLSE into the sum of the two components $A(z,t)$ and $a(z,t)$. $A(z,t)$ is the deterministic time- and z-varying ensemble-averaged mean for the solution, and $a(z,t)$ is the zero-mean stochastic perturbation. Next, we describe formulations for computing the second-order probabilistic characterizations, i.e., ensemble-averaged time-varying variance, correlation function and spectral density, for the perturbation $a(z,t)$.

3.2. Covariance matrix formulation for perturbation analysis

We start by discretizing time t with N_t time points $t_1, t_2, \ldots, t_{N_t-1}, t_{N_t}$ which are not necessarily equispaced. We define the column vectors

$$\begin{aligned}\mathbf{a}_c(z) &= [a(z,t_1)\ a(z,t_2)\cdots a(z,t_{N_t})]^{\mathrm{T}}, \\ \mathbf{A}_c(z) &= [A(z,t_1)\ A(z,t_2)\ldots A(z,t_{N_t})]^{\mathrm{T}},\end{aligned} \tag{5}$$

where the bold characters and the subscript c denote that $\mathbf{a}_c(z)$ and $\mathbf{A}_c(z)$ are complex-valued *vector* functions of z. The time dependence has disappeared because of the collocation points we have introduced. We separate $\mathbf{a}_c(z)$ and $\mathbf{A}_c(z)$ into their real and imaginary parts

$$\mathbf{a}_c(z) = \mathbf{a}_r(z) + \mathrm{j}\mathbf{a}_i(z), \quad \mathbf{A}_c(z) = \mathbf{A}_r(z) + \mathrm{j}\mathbf{A}_i(z) \tag{6}$$

and form the real-valued long column vectors

$$\mathbf{a}(z) = \begin{bmatrix}\mathbf{a}_r(z)^{\mathrm{T}} & \mathbf{a}_i(z)^{\mathrm{T}}\end{bmatrix}^{\mathrm{T}}\mathbf{A}(z) = \begin{bmatrix}\mathbf{A}_r(z)^{\mathrm{T}} & \mathbf{A}_i(z)^{\mathrm{T}}\end{bmatrix}^{\mathrm{T}}. \tag{7}$$

We define

$$\mathbb{A}(z) = \begin{bmatrix} -2\mathscr{D}[\mathbf{A}_r(z)]\mathscr{D}[\mathbf{A}_i(z)] & -\mathscr{D}[\mathbf{A}_r(z)]^2 - 3\mathscr{D}[\mathbf{A}_i(z)]^2 \\ 3\mathscr{D}[\mathbf{A}_r(z)]^2 + \mathscr{D}[\mathbf{A}_i(z)]^2 & 2\mathscr{D}[\mathbf{A}_r(z)]\mathscr{D}[\mathbf{A}_i(z)]\end{bmatrix}, \tag{8}$$

$$\mathbb{B}_2 = \begin{bmatrix} 0 & \mathbb{D}_2 \\ -\mathbb{D}_2 & 0\end{bmatrix}, \quad \mathbb{B}_3 = \begin{bmatrix} \mathbb{D}_3 & 0 \\ 0 & \mathbb{D}_3\end{bmatrix}, \tag{9}$$

where $\mathbb{D}_2$ and $\mathbb{D}_3$ are second-order and third-order differentiation operators (or matrices) in time, and $\mathscr{D}[\cdot]$ is a diagonal operator (or a diagonal matrix with the elements of the argument vector on the main diagonal). At this point, we do not make any assumptions on how the time differentiation operators $\mathbb{D}_2$ and $\mathbb{D}_3$ are implemented.

With the collocation for t introduced above and using Eqs. (7)–(9), the linear(ized) perturbation PDE in (4) can be transformed into

$$\frac{\mathrm{d}\mathbf{a}(z)}{\mathrm{d}z} = -\frac{1}{2}\alpha\mathbf{a}(z) + \frac{1}{2}\beta_2\mathbb{B}_2\mathbf{a}(z) + \frac{1}{6}\beta_3\mathbb{B}_3\mathbf{a}(z) + \gamma\mathbb{A}(z)\mathbf{a}(z). \tag{10}$$

Now we form

$$\frac{\mathrm{d}\left[\mathbf{a}(z)\mathbf{a}(z)^{\mathrm{T}}\right]}{\mathrm{d}z} = \frac{\mathrm{d}\mathbf{a}(z)}{\mathrm{d}z}\mathbf{a}(z)^{\mathrm{T}} + \mathbf{a}(z)\frac{\mathrm{d}\mathbf{a}(z)^{\mathrm{T}}}{\mathrm{d}z} \tag{11}$$

and let $\mathbf{K}(z)$ be the z-dependent *covariance matrix* for the time-collocated stochastic perturbation

$$\mathbf{K}(z) = \mathbb{E}\left[\mathbf{a}(z)\mathbf{a}(z)^{\mathrm{T}}\right], \tag{12}$$

where $\mathbb{E}[\cdot]$ denotes the probabilistic "expectation" operator. Note that $\mathbf{K}(z)$ is a real and symmetric matrix. Then, we substitute (10) in (11), take the expectation of both sides, and obtain

$$\begin{aligned}\frac{\mathrm{d}\mathbf{K}(z)}{\mathrm{d}z} = &-\alpha\mathbf{K}(z) + \frac{1}{2}\beta_2\left[\mathbb{B}_2\mathbf{K}(z) + \mathbf{K}(z)\mathbb{B}_2^{\mathrm{T}}\right] + \frac{1}{6}\beta_3\left[\mathbb{B}_3\mathbf{K}(z) + \mathbf{K}(z)\mathbb{B}_3^{\mathrm{T}}\right] \\ &+ \gamma\left[\mathbb{A}(z)\mathbf{K}(z) + \mathbf{K}(z)\mathbb{A}(z)^{\mathrm{T}}\right],\end{aligned} \tag{13}$$

which is a system of *linear* differential equations for the *covariance matrix* of the time-collocated stochastic perturbation. We will refer to this equation as COVODE during the rest of our treatment. Note that even though $\mathbb{B}_2$ and $\mathbb{B}_3$ above do not depend on z, $\mathbb{A}(z)$ is a *z-varying* coefficient matrix which can be calculated by substituting $A(z,t)$ in (8). By solving the system of differential equations above, one can compute the noise covariance matrix $\mathbf{K}(z=L)$ at the end of the fiber link given an initial launch condition $\mathbf{K}(z=0)$. The numerical computation of $\mathbf{K}(z)$ is described in Section 4. Note that the stochastic perturbation $a(z,t)$ is, in general, a *non-stationary* stochastic process as a function of time t, which is captured by the covariance matrix formalism described above.

The noisy perturbation exerted on the system can enter (13) in various ways, as an additional forcing term or as a non-zero initial condition $\mathbf{K}(z=0)$. For our application, we are mainly interested in forcing terms in the form $\mathbf{F}\delta(z_f)$, where $\delta(z_f)$ is the Dirac's delta function situated at $z=z_f$. In fact, a non-zero initial condition $\mathbf{K}(z=0)$ can be considered as a forcing term in the form $\mathbf{F}\delta(z_f)$ where $z_f=0$ and $\mathbf{F}=\mathbf{K}(z=0)$ and a zero initial condition. Forcing terms in this form model localized, lumped (along the propagation direction at $z=z_f$) perturbations to the system. One could also consider distributed perturbations and introduce them into (13) as a general z-dependent forcing term in the form $\mathbf{P}(z)$. The t dependence of the stochastic characteristics of the perturbation or noise influencing the system are captured by the matrices $\mathbf{F}$ or $\mathbf{P}(z)$ above. For example, if these are diagonal matrices then the time samples of noise are uncorrelated with each other and hence modeling a white noise excitation on the system. If the values on the diagonal are all the same then this would be model for stationary white noise, and if they are different then a model for non-stationary white noise. In general, with a full matrix with a non-constant diagonal, one can model non-stationary colored noise excitations on the system.

3.3. Frequency-decomposed formulation for perturbation analysis

We now describe an alternative, frequency-decomposed formulation for the characterization of the stochastic perturbation $a(z,t)$, which *complements* the covariance matrix formulation described above.

Note: If you have not read Section 2, you can skip the rest of this paragraph in italics. *This formulation can be considered as a generalization of the "transfer matrix" approach presented in* [17], *where the authors consider the propagation of a comb of unmodulated carriers, together with optical noise. The "transfer matrix" they compute is composed of transfer functions from the noise sidebands of every optical carrier to the noise*

sidebands of all the other carriers in the comb. These sideband transfer functions can be interpreted as follows: If one injects a "small" CW (continuous-wave, meaning unmodulated) signal (tone) at a frequency (at $z = 0$ into the fiber along with the large CW carriers for the channels) that is ω offset from a chosen carrier/channel, then at $z = L$ along the fiber, "small" CW signals (tones) ω offset from all of the carriers will appear. The sideband transfer functions quantify the ratio of the magnitude of these generated tones to the one that was injected. The frequency-decomposed formulation we will present next, is essentially a generalization of the sideband transfer matrix approach to modulated carriers. Authors in [17] *assumed that the noise around every carrier is a narrowband signal, and the noise sidebands of neighboring carriers do not overlap. Through this assumption, the total optical noise surrounding all the carriers can be decomposed into noise components around every carrier. Even though the total optical noise surrounding all the carriers is non-stationary, the noise components around the individual carriers becomes stationary for unmodulated carriers. Hence, the authors in* [17] *ingeniously dodged away from having to deal with non-stationary processes and time-varying transfer functions. However, for the treatment of the most general case with modulated carriers, non-stationarity and time-varyingness is unavoidable.*

A (non-stationary) (Gaussian) stochastic process $x(t)$, i.e., noise signal, can be represented in frequency-decomposed form by the following formal integral:

$$x(t) = \int_{-\infty}^{\infty} X(t,f)\exp(\mathrm{j}2\pi ft)\xi(f)\,\mathrm{d}f, \tag{14}$$

where $\xi(f)$ is a stationary white Gaussian process as a function of f. $X(t,f)$ is a deterministic complex quantity. If $x(t)$ is stationary, then $X(t,f)$ becomes independent of time t, and $|X(t,f)|^2$ is then the spectral density of $x(t)$.

The representation in (14) for a non-stationary stochastic process will be very useful in the derivation of the alternative frequency-decomposed formulation for perturbation/noise analysis. However, the variances of, and the correlations among, the noise/perturbation time samples are not readily available in this representation, which are the desired stochastic characterizations in most applications. [8] The variances of, and the correlations among, the noise samples are directly available from the noise covariance matrices produced by the covariance matrix formulation. One can compute them using the frequency-decomposed representation in (14) as follows:

$$\mathbb{E}\left[x(t_1)x(t_2)^{\star}\right] = \int_{-\infty}^{\infty} X(t_1,f)X(t_2,f)^{\star}\exp(\mathrm{j}2\pi f(t_1-t_2))\,\mathrm{d}f. \tag{15}$$

The equation above follows from (14) using the fact that $\xi(f)$ in (14) is white and hence delta-correlated, i.e.,

$$\mathbb{E}[\xi(f_1)\xi(f_2)] = \delta(f_1 - f_2). \tag{16}$$

For the computation of the variances and correlations of the noise samples using (15), one needs to compute the noise representation $X(t,f)$ for a range of frequencies f where the magnitude of $X(t,f)$ is significant.

[8] For example, variances and correlations are needed for communication system BER performance evaluation. To see why that is the case, we need to consider what the electronic receiver exactly does with the signal impinges on it in a digital optical fiber communication system. The electronic receiver at the end of the fiber link *samples* the received signal once every symbol period, at time instants determined by the clock recovery circuitry. Then, the detector makes a decision on which symbol has been sent by the transmitter, making "occasional errors" due to noise and other non-idealities. In evaluating the decision error rate of the detector, a stochastic characterization of the noise samples is needed. For simple detectors, the stochastic characterization needed is just the variances of the noise samples. For more complicated/advanced detectors the correlations between noise samples may also be needed.

Next, we use the frequency-decomposed representation in (14) for the stochastic perturbation $a(z,t)$, in which case, the representation becomes also a function of z. Below, we replace the real frequency variable f with the complex frequency variable s. We substitute

$$a_r(z,t) = h_r(z,t,s)\exp(st), \quad a_i(z,t) = h_i(z,t,s)\exp(st) \tag{17}$$

in (4), divide both sides of the equation by $\exp(st)$ and obtain

$$\begin{aligned}\frac{\mathrm{d}}{\mathrm{d}z}\begin{bmatrix} h_r(z,t,s) \\ h_i(z,t,s)\end{bmatrix} &= -\frac{1}{2}\alpha\begin{bmatrix} h_r(z,t,s) \\ h_i(z,t,s)\end{bmatrix} + \frac{1}{2}\beta_2\left(\frac{\partial^2}{\partial t^2} + 2s\frac{\partial}{\partial t} + s^2\right)\begin{bmatrix} 0 & 1 \\ -1 & 0\end{bmatrix}\begin{bmatrix} h_r(z,t,s) \\ h_i(z,t,s)\end{bmatrix} \\ &\quad + \frac{1}{6}\beta_3\left(\frac{\partial^3}{\partial t^3} + 3s\frac{\partial^2}{\partial t^2} + 3s^2\frac{\partial}{\partial t} + s^3\right)\begin{bmatrix} 1 & 0 \\ 0 & 1\end{bmatrix}\begin{bmatrix} h_r(z,t,s) \\ h_i(z,t,s)\end{bmatrix} \\ &\quad + \gamma\begin{bmatrix} -2A_r(z,t)A_i(z,t) & -A_r(z,t)^2 - 3A_i(z,t)^2 \\ 3A_r(z,t)^2 + A_i(z,t)^2 & 2A_r(z,t)A_i(z,t)\end{bmatrix}\begin{bmatrix} h_r(z,t,s) \\ h_i(z,t,s)\end{bmatrix}.\end{aligned} \tag{18}$$

We introduce the collocation points in t as in (5) and define the vector

$$\mathbf{h}(z,s) = [h_r(z,t_1,s)\cdots h_r(z,t_{N_t},s),\ h_i(z,t_1,s)\cdots h_i(z,t_{N_t},s)]^{\mathrm{T}}. \tag{19}$$

With (19), and $\mathbf{A}_r(z)$ and $\mathbf{A}_i(z)$ as in (6), and with

$$\begin{aligned}\mathbf{R}(z) &= \gamma\begin{bmatrix} -2\mathscr{D}[\mathbf{A}_r(z)]\mathscr{D}[\mathbf{A}_i(z)] & -\mathscr{D}[\mathbf{A}_r(z)]^2 - 3\mathscr{D}[\mathbf{A}_i(z)]^2 \\ 3\mathscr{D}[\mathbf{A}_r(z)]^2 + \mathscr{D}[\mathbf{A}_i(z)]^2 & 2\mathscr{D}[\mathbf{A}_r(z)]\mathscr{D}[\mathbf{A}_i(z)]\end{bmatrix}, \\ \mathbf{S}_0 &= \begin{bmatrix} -\frac{1}{2}\alpha\mathbf{I} + \frac{1}{6}\beta_3\mathbb{D}_3 & \frac{1}{2}\beta_2\mathbb{D}_2 \\ -\frac{1}{2}\beta_2\mathbb{D}_2 & -\frac{1}{2}\alpha\mathbf{I} + \frac{1}{6}\beta_3\mathbb{D}_3\end{bmatrix}, \quad \mathbf{S}_3 = \frac{1}{6}\beta_3\mathbf{I}, \\ \mathbf{S}_1 &= \begin{bmatrix} \frac{1}{2}\beta_3\mathbb{D}_2 & \beta_2\mathbb{D}_1 \\ -\beta_2\mathbb{D}_1 & \frac{1}{2}\beta_3\mathbb{D}_2\end{bmatrix}, \quad \mathbf{S}_2 = \frac{1}{2}\begin{bmatrix} \beta_3\mathbb{D}_1 & \beta_2\mathbf{I} \\ -\beta_2\mathbf{I} & \beta_3\mathbb{D}_1\end{bmatrix}.\end{aligned} \tag{20}$$

(18) can be expressed as

$$\frac{\mathrm{d}}{\mathrm{d}z}\mathbf{h}(z,s) = \left[\mathbf{R}(z) + \mathbf{S}_0 + s\mathbf{S}_1 + s^2\mathbf{S}_2 + s^3\mathbf{S}_3\right]\mathbf{h}(z,s). \tag{21}$$

Given an initial launch condition $\mathbf{h}(0,s)$, one can solve (21) (referred to as FDODE from now on) above for $\mathbf{h}(z=L,s)$ for a range of frequencies $s = \mathrm{j}2\pi f$. [9] However, one has to solve (21) for every value of $s = \mathrm{j}2\pi f$ that is of interest. We will now put (21) in a form that is amenable to the use of efficient *reduced-order modeling* (ROM) *techniques* [19,20] for the computation of the frequency dependence of $\mathbf{h}(z=L,s)$, where one does not have to solve (21) repeatedly for every frequency $s = \mathrm{j}2\pi f$ of interest. [10] The form for the output $\mathbf{h}(z=L,s)$ that will be produced by the algorithm can also be used as its input, i.e., $\mathbf{h}(z=0,s)$.

We introduce the collocation points $z = z_0, z_1, \ldots, z_M$

$$\mathfrak{h}(s) = [\mathbf{h}(z_1,s), \ldots, \mathbf{h}(z_M,s)]^{\mathrm{T}}, \tag{22}$$

[9] Please see the end of Section 3.2 for a discussion of how one would introduce the noisy perturbation into (21).

[10] The form that we will derive is also useful for noise analysis of cascaded chains of amplified fiber spans for a long-haul optical fiber communication link.

where $z_0 = 0$ and $z_M = L$. We then apply a (multistep) integration formula to the system of ODEs in (21)

$$\left[\mathbb{Z}_0 + s\mathbb{Z}_1 + s^2\mathbb{Z}_2 + s^3\mathbb{Z}_3\right]\mathfrak{h}(s) = \mathbb{R}\mathbf{h}(0,s) \tag{23}$$

where the matrices $\mathbb{Z}_i$ and $\mathbb{R}$ depend on the specific integration formula used for the system of ODEs in (21). Given the "initial" condition $\mathbf{h}(0,s)$, we would like to compute $\mathbf{h}(L,s)$. Then,

$$\mathbf{h}(L,s) = \mathbb{L}^{\mathrm{T}}\mathfrak{h}(s), \tag{24}$$

where $\mathbb{L} = [\mathbf{0}\cdots\mathbf{0}\mathbf{I}]^{\mathrm{T}}$ selects the vector $\mathbf{h}(z_M,s)$ out of the "long" vector $\mathfrak{h}(s)$. Hence,

$$\mathbf{h}(L,s) = \mathbb{L}^{\mathrm{T}}\left[\mathbb{Z}_0 + s\mathbb{Z}_1 + s^2\mathbb{Z}_2 + s^3\mathbb{Z}_3\right]^{-1}\mathbb{R}\mathbf{h}(0,s), \tag{25}$$

where $\mathbb{Z}_i$ are $N_tN_z \times N_tN_z$, $\mathbb{L}$ and $\mathbb{R}$ are $N_tN_z \times N_t$. N_t is the number of time collocation points, and N_z is the number of z-steps. We assume that the initial launch condition $\mathbf{h}(0,s)$ is given as a rational matrix function of s

$$\mathbf{h}(0,s) = \mathbb{L}_{ic}^{\mathrm{T}}[\mathbf{I} - s\mathbb{T}_{ic}]^{-1}\mathbb{R}_{ic}. \tag{26}$$

We now put (25) and (26) together and rewrite (25) as follows, in a form suitable for ROM-based s-dependence computation

$$\mathbf{h}(L,s) = \mathscr{L}^{\mathrm{T}}[\mathscr{G} + s\mathscr{C}]^{-1}\mathscr{R}, \tag{27}$$

where

$$\mathscr{L} = [\mathbf{0} \quad \mathbb{L}^{\mathrm{T}} \quad \mathbf{0} \quad \mathbf{0}]^{\mathrm{T}}, \quad \mathscr{R} = \left[\mathbb{R}_{ic}^{\mathrm{T}} \quad \mathbf{0} \quad \mathbf{0} \quad \mathbf{0}\right]^{\mathrm{T}},$$
$$\mathscr{G} + s\mathscr{C} = \begin{bmatrix} \mathbf{I} - s\mathbb{T}_{ic} & \mathbf{0} & \mathbf{0} & \mathbf{0} \\ -\mathbb{R}\mathbb{L}_{ic}^{\mathrm{T}} & \mathbb{Z}_0 + s\mathbb{Z}_1 & s\mathbb{Z}_2 & s\mathbb{Z}_3 \\ \mathbf{0} & s\mathbf{I} & -\mathbf{I} & \mathbf{0} \\ \mathbf{0} & \mathbf{0} & s\mathbf{I} & -\mathbf{I} \end{bmatrix}. \tag{28}$$

Hence

$$\mathscr{G} = \begin{bmatrix} \mathbf{I} & \mathbf{0} & \mathbf{0} & \mathbf{0} \\ -\mathbb{R}\mathbb{L}_{ic}^{\mathrm{T}} & \mathbb{Z}_0 & \mathbf{0} & \mathbf{0} \\ \mathbf{0} & \mathbf{0} & -\mathbf{I} & \mathbf{0} \\ \mathbf{0} & \mathbf{0} & \mathbf{0} & -\mathbf{I} \end{bmatrix}, \quad \mathscr{C} = \begin{bmatrix} \mathbb{T}_{ic} & \mathbf{0} & \mathbf{0} & \mathbf{0} \\ \mathbf{0} & \mathbb{Z}_1 & \mathbb{Z}_2 & \mathbb{Z}_3 \\ \mathbf{0} & \mathbf{I} & \mathbf{0} & \mathbf{0} \\ \mathbf{0} & \mathbf{0} & \mathbf{I} & \mathbf{0} \end{bmatrix}. \tag{29}$$

We will refer to (27) as FDROM during the rest of our treatment.

4. Numerical methods and implementation

In this section, we will describe the numerical solution of

- Eq. (1) (NLSE) for the deterministic mean of the solution of SNLSE, in Section 4.1.
- Eq. (13) (COVODE) for the covariance matrix of the time-collocated zero-mean noise, i.e., stochastic perturbation, in Section 4.2.
- Eq. (21) (FDODE) and (27) (FDROM) for the frequency-decomposed representation of noise, in Section 4.3.

4.1. Numerical solution of NLSE

Eq. (1) is a PDE which combines a low-order (zeroth) non-linear term with higher-order (second and third) linear terms. To obtain efficient and accurate numerical solutions for such PDEs, it is desirable to use high-order approximations in space z and time t [21]. Spectral methods offer very high *time* resolution for (1) [13,14]. Once the time part of (1) is spectrally discretized and the resulting system of ordinary differential equations (ODEs) is transformed into the spectral domain, one obtains

$$\frac{\mathrm{d}}{\mathrm{d}z}\hat{\mathbf{A}}(z) = L\hat{\mathbf{A}}(z) + N\left[\hat{\mathbf{A}}(z)\right], \tag{30}$$

where N is a non-linear operator, and L is a diagonal matrix (operator). L has widely varying values on the diagonal, since the diagonal elements are the summation of a quadratic and cubic function of the frequency variable (due to second- and third-order dispersion). Hence, the linear part of the system of ODEs in (30) is *stiff*. This stiffness combined with the non-linearity in (30) precludes the use of high-order schemes for z-integration because of severe stability restrictions [14,21]. The stability restriction imposes an upper limit on the size of the z-steps that can be taken.

L in (30) (which is in the spectral domain) is diagonal and can be applied trivially. However, the non-linear operator N in (30) needs to be implemented in the time-domain, this requires two FFTs, one to go back to the time-domain and another one to come back to the spectral domain. The non-linear operator N is diagonal in the time-domain.

In the optical fiber communication community, the z-stepping method of choice is the so-called *split-step* method [13], an *explicit* z-stepping scheme based on operator splitting. When a sufficiently small step size is not used with this method, inaccuracies due to instability in numerical integration manifests itself as induced spurious tones, which are called *fictitious four-wave mixing* in the photonics literature [22].

If an *implicit* scheme is used for z-stepping, larger steps can be taken compared with an explicit scheme. However, even implicit z-stepping may suffer from (milder) stability restrictions on the step size when high-orders are used. One may be limited by a second-order A-stable scheme, e.g., trapezoidal formula. Moreover, an implicit scheme applied to (30) requires the solution of a *system of non-linear equations* at every z-step.

The idea behind the *linearly implicit* schemes [14,21] arises from the observation that the stiffness in (30) is due to the *linear* part, and hence one can use an implicit (possibly A-stable) multi-step formula to advance the linear part and an explicit high-order scheme to advance the non-linear part. Then, the step-size would become accuracy-limited and not stability-limited. Moreover, the solution of only a *linear* system of equations at every step would be needed. L in (30) is *diagonal* when time discretization is done with a spectral method, and hence the linear system of equations that need to be solved at every z-step is diagonal and has a trivial solution.

Fornberg and Driscoll [14] describe an extension of the linearly implicit scheme above. In addition to applying separate explicit and implicit integration methods for the non-linear and the linear part, they also split the linear part into *low, medium* and *high* Fourier wavenumber regions. These wavenumber regions correspond to *slow*, *medium* and *fast* time scales. In the *slider* method they propose, they use a different integration scheme for each (Fourier wavenumber) region in the linear part. For the low Fourier wavenumber region, they use the same explicit high-order scheme used for the non-linear part. In one version of the slider method, Fornberg and Driscoll [14] use low: *AB7*/*AB7*, medium: *AB7*/*AM6* and high: *AB7*/*AM2** for the (*non-linear*/*linear* part where *ABk* is the explicit kth order Adams–Bashfort formula, and *AMk* is the implicit kth order Adams–Moulton formula. The diagonal linear term L in (30) has a complex spectrum with a very small real part compared with the imaginary part. The (frequency-independent) real part is due to the loss of the fiber, and the (strongly frequency-dependent)

imaginary part is due to second- and third-order dispersion. The boundaries between the low, medium, and high Fourier wavenumber regions are determined by the extent of the stability regions along the imaginary axis for the integration schemes used for the linear part. *AM2** above is a modified second-order formula, which is given by

$$\hat{\mathbf{A}}_{n+1} - \hat{\mathbf{A}}_n = \frac{h}{2}\left(\frac{3}{2}L\hat{\mathbf{A}}_{n+1} + \frac{1}{2}L\hat{\mathbf{A}}_{n-1}\right) \tag{31}$$

when constant step sizes are used, with h as the z-step size [14]. Note that (31) is a *two-step* second-order formula in contrast with the one-step second-order *AM2* (trapezoidal rule). It has an error constant of $1/3$ compared with $1/12$ for *AM2*. However, its stability region (Fig. 2) extends into the right-half-plane covering the imaginary axis. Fornberg and Driscoll [14] propose *AM2** in place of *AM2* for problems with almost a purely imaginary spectrum. We have implemented a self-starting, fully variable step size version of Fornberg and Driscoll's linearly implicit slider method outlined above for the numerical solution of (1): NLSE for the deterministic multi-channel modulated optical signal. Automatic step size control is performed based on an estimation of the local truncation error [23]. Commonly used step size selection heuristics [23], as well as new ones we found to be useful that are specific to the linearly implicit slider scheme described above, have been implemented in our code. The new heuristics are involved with the coordination of truncation error computation and step size selection in the presence of different integration

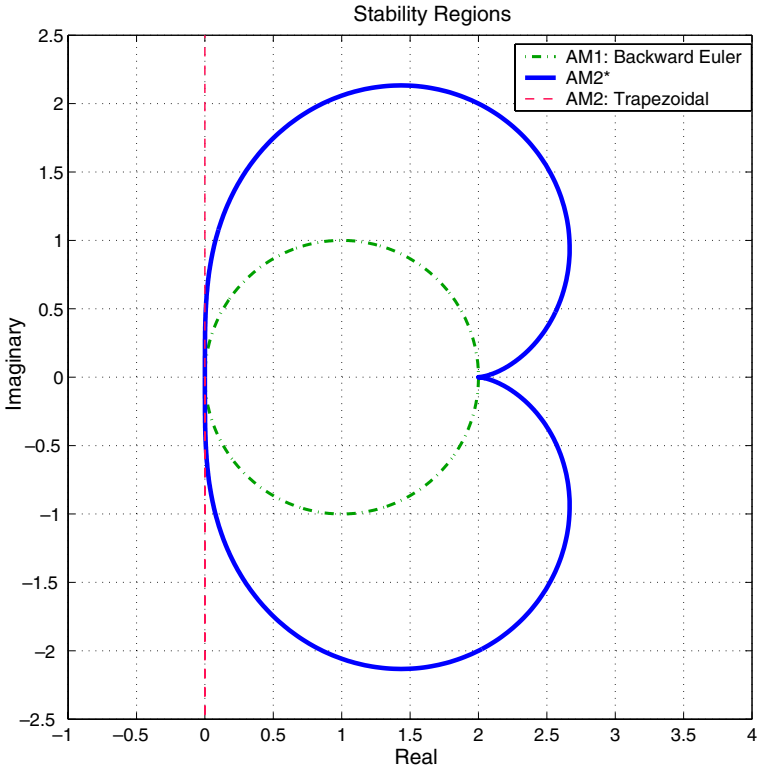

Fig. 2. Stability region for *AM2**.

schemes being used for the linear and non-linear parts of (30) and also for the low, medium and high Fourier wavenumber regions of the linear part.

The numerical solution of NLSE has a computational complexity of $O(N_z N_f \log N_f)$, where N_f is the number of Fourier modes used in the spectral representation, and N_z is the number of z-steps. The storage complexity is $O(N_f)$.

For a comparison of the split-step method and the linearly implicit schemes as well as other integration schemes for solving stiff non-linear PDEs of the form in (30), please see [14,21].

4.2. Numerical solution of COVODE

In contrast with the non-linear NLSE: (1), COVODE: (13) is a linear system of equations. The right-hand side (RHS) of COVODE has terms which have z-independent coefficient matrices. These arise from the linear loss and dispersion terms in the original NLSE. RHS of COVODE also has terms with z-dependent coefficient matrices. These terms arise from the non-linear term in the original NLSE. COVODE is closely related to NLSE, and the same stiffness properties carry over. Hence, we use the same linearly implicit slider schemes (described above) for the numerical integration of COVODE. In the context of COVODE, it is not exactly accurate to call the integration schemes as linearly implicit, because all terms in COVODE are linear. To be precise, we use implicit sliding schemes for the medium and high wavenumber loss and dispersion terms in COVODE, and use explicit high-order, e.g., *AB7*, schemes for the low wavenumber loss and dispersion terms and the z-varying linear terms due to the non-linearity of the fiber. Application of the "linearly" implicit integration schemes to COVODE in (13) is straightforward, except for some tinkering required on how to apply the sliding scheme with a partition of slow, medium and fast time scales.

We solve COVODE in (13) using the same spectral discretization for time t that we use for NLSE. We first transform (13) into the spectral domain. Then, the coefficient matrices $\mathbb{B}_2$ and $\mathbb{B}_3$ are given by (9) where $\mathbb{D}_2$ and $\mathbb{D}_3$ are now diagonal matrices.

For COVODE, we use the same z-stepping scheme and the same z-steps that is used and automatically selected for NLSE. At every z-step, we first compute the solution of NLSE, $\mathbf{A}_c(z) = \mathbf{A}_r(z) + \mathrm{j}\mathbf{A}_i(z)$, which is needed to evaluate the z-varying coefficient matrix $\mathbb{A}(z)$ for COVODE in (8). In the spectral domain, the evaluation of the term involving $\mathbb{A}(z)$ in COVODE requires the use of FFTs. When we apply an explicit multistep scheme to the z-varying terms involving $\mathbb{A}(z)$ in COVODE, and an implicit scheme to the loss and dispersion terms involving α, $\mathbb{D}_2$ and $\mathbb{D}_3$, we need to solve a matrix equation, at every z-step, of the form given by

$$\mathbf{E}\,\mathbf{K}_f(z_n) + \mathbf{K}_f(z_n)\,\mathbf{E}^\dagger = \mathbf{F}(z_n), \tag{32}$$

where † denotes conjugate-transpose, and

$$\mathbf{E} = \begin{bmatrix} \mathbf{D}_d & \mathbf{D}_o \\ -\mathbf{D}_o & \mathbf{D}_d \end{bmatrix} \tag{33}$$

where $\mathbf{D}_d$ and $\mathbf{D}_o$ are z-independent diagonal matrices. The subscript $_f$ for $\mathbf{K}_f(z_n)$ denotes that we are in the spectral domain. (32) is a Lyapunov matrix equation [24]. A direct-method solution of the Lyapunov matrix equation using the Bartels–Stewart algorithm is $O(N_f^3)$ [25]. However, since the coefficient matrix $\mathbf{E}$ is in a very special form, we do not need to use the Bartels–Stewart algorithm which is meant to handle arbitrary coefficient matrices. When $\mathbf{E}$ is in the form given by (33), (32) can be solved with a specialized algorithm that is $O(N_f^2)$, which we outline next.

From (32) with $\mathbf{E}$ as in (33), one can write a system of equations for two columns of $\mathbf{K}_f(z_n)$ at a time. The coefficient matrix for these equations has the form

$$\mathbf{E}_2 = \begin{bmatrix} \mathbf{E} + c\mathbf{I} & d\mathbf{I} \\ -d\mathbf{I} & \mathbf{E} + c\mathbf{I} \end{bmatrix}, \tag{34}$$

where c and d are the conjugates of two of the entries of $\mathbf{D}_d$ and $\mathbf{D}_o$. The inverse of this matrix is given by

$$\mathbf{E}_2^{-1} = \begin{bmatrix} \mathbf{G}^{-1} & \mathbf{0} \\ \mathbf{0} & \mathbf{G}^{-1} \end{bmatrix} \begin{bmatrix} \mathbf{E} + c\mathbf{I} & -d\mathbf{I} \\ d\mathbf{I} & \mathbf{E} + c\mathbf{I} \end{bmatrix}, \tag{35}$$

where

$$\mathbf{G} = \left((\mathbf{E} + c\mathbf{I})^2 + d^2\mathbf{I} \right). \tag{36}$$

The structure in (33) is preserved under the operations of matrix addition, matrix square, matrix inverse and the addition of a multiple of the identity matrix $\mathbf{I}$. Thus, $\mathbf{E} + c\mathbf{I}$, $(\mathbf{E} + c\mathbf{I})^2$ and $(\mathbf{E} + c\mathbf{I})^2 + d^2\mathbf{I}$ above are all exactly in the same form as $\mathbf{E}$ in (33). Hence, the inverse of $(\mathbf{E} + c\mathbf{I})^2 + d^2\mathbf{I}$ can also be computed easily. The inverse of a matrix of the form in (33) is given by

$$\mathbf{E}^{-1} = \begin{bmatrix} \left(\mathbf{D}_d^2 + \mathbf{D}_o^2\right)^{-1} & \mathbf{0} \\ \mathbf{0} & \left(\mathbf{D}_d^2 + \mathbf{D}_o^2\right)^{-1} \end{bmatrix} \begin{bmatrix} \mathbf{D}_d & -\mathbf{D}_o \\ \mathbf{D}_o & \mathbf{D}_d \end{bmatrix}. \tag{37}$$

The special structure of the coefficient matrix $\mathbf{E}$ above is due to the fact that we are using an implicit integration scheme *only* for the loss and dispersion terms of COVODE, and that the solution is performed in the spectral domain with a spectral discretization of time t.

With a flat and unstructured representation for the covariance matrix, it is not possible to reduce the computational complexity of the solution of (32) below $\mathrm{O}(N_f^2)$. If the stochastic perturbation is a stationary process, then the covariance matrix in the spectral domain is diagonal, and in the time domain it is Hermitian and Toeplitz. [11] Hence, it is structured and can be represented with $\mathrm{O}(N_f)$ numbers as opposed to $\mathrm{O}(N_f^2)$ numbers. However, in general, the stochastic perturbation is non-stationary, and there is no apparent exact structure in the covariance matrix. Still, it is worthwhile to investigate if there is any (numerically approximate) special structure that arises in the noise covariance matrices and how it can be exploited for efficient representation and computation. With an unstructured, flat representation for the covariance matrix, the computational complexity for the numerical solution of COVODE is $\mathrm{O}(N_z N_f^2 \log N_f)$, the storage complexity is $\mathrm{O}(N_f^2)$.

We have implemented the above outlined method for the numerical solution of COVODE: (13) along with the numerical solution of NLSE: (1). Noise analysis examples generated using this implementation and a discussion of system performance evaluation using the noise analysis results is in Section 5.

4.3. Numerical solution and evaluation of FDODE and FDROM

FDODE: (21) is a system of linear ODEs for the frequency-decomposed representation of the stochastic perturbation, i.e., optical noise. For a given value of frequency $s = \mathrm{j}2\pi f$, the numerical solution of FDODE can be performed, again, by using the linearly implicit schemes described above. The terms that arise due to fiber loss and dispersion, $s^i\mathbf{S}_i$, $i = 0, \ldots, 3$ in (21), are advanced with implicit sliding schemes. The term due

[11] A Toeplitz matrix is a matrix whose entries are constant on each diagonal.

to non-linearity, $\mathbf{R}(z)$ in (21), is advanced with an explicit scheme. When FDODE is transformed into the spectral domain, the linear system of equations that need to be solved at every z-step, also has a coefficient matrix of the form in (33) and can be trivially solved with $O(N_f)$ operations using the matrix inverse in (37). Note that, however, we do not obtain a Lyapunov matrix equation when FDODE is discretized, it is just a regular linear system of equations. The computational complexity of the solution of (21) is $O(N_z N_s N_f \log N_f)$ where N_s is the number of grid points in $s = j2\pi f$ that needs to be computed. The storage complexity is $O(N_s N_f)$.

The noise sample variances and correlations are computed using (a discretized version of) the integral in (15). For an accurate noise characterization, the integral in (15) needs to be computed over the whole range of the frequencies f used in the spectral representation of the signals and noise. Thus, we need to evaluate FDODE for a range of grid points in $s = j2\pi f$ that covers the whole spectrum that is used in the spectral representations. For simplicity and efficiency in computations, we choose this grid to be the *same* frequency grid used for the Fourier modes in the signal spectral representation, i.e., $N_s = N_f$. Hence, the computational and storage complexity of the numerical solution of FDODE is the same as that of the numerical solution of COVODE. However, the evaluation of FDODE for a number of grid points can be parallelized easily to run on a cluster of computers. Evaluations for different values of $s = j2\pi f$ are totally independent of each other, and hence this is an "embarrasingly parallel" operation.

With the ROM-based formulation FDROM: (27), one can compute the s-dependence of $\mathbf{h}(z = L, s)$ in (27) in approximate (Padé approximation) analytical (rational) form. A detailed description of reduced-order modeling and the numerical methods involved is beyond the scope of this paper, and the reader is referred to [19,20,26] for a detailed discussion. With the ROM-based approach one needs to solve systems of linear equations with $\mathsf{G} + s\mathsf{C}$ in (28) at an expansion point $s = s_0$, where the expansion point is for the Padé approximation that will be computed for the rational function $\mathbf{h}(z = L, s)$ of s in (27). Solving a linear system of equations with $\mathsf{G} + s\mathsf{C}$ as the coefficient matrix corresponds to solving versions of (21) from $z = 0$ to $z = L$. We again use the linearly implicit schemes for this computation as described before. If we assume that the number of iterations needed in the ROM-based approach is much fever than the size of the problem [26], the computational complexity of the ROM-based evaluation of FDROM in (27) is $O(N_z N_f \log N_f)$. The storage complexity is $O(N_z N_f)$. The ROM-based approach can potentially reduce the computational cost of noise analysis significantly.

We have implemented the numerical solution of FDODE: (21) outlined above. Noise analysis examples that will be presented in Section 5 were also run using this implementation for the frequency-decomposed formulation. As expected, we obtained the same results as the covariance matrix formulation produced. This implementation is parallelizable as opposed to the implementation for the numerical solution of COVODE: (13). Moreover, the frequency-decomposed formulation offers further potentially significant computational benefits in the ROM-based form in FDROM. The implementation of the parallelized version of the numerical solution of FDODE: (21) and the ROM-based evaluation of FDROM is part of the current/future work.

5. Practical results and discussion

In this section, we report results using the formulations, computational techniques and the implementations described throughout the paper. More specifically, the results that will be presented here have been obtained from the numerical solutions of NLSE: (1), COVODE: (13) and FDODE: (21). These equations are solved using a spectral discretization for the time variable t with a Fourier basis, as explained in Section 4. Note that, as explained in Sections 4.2 and 4.3, COVODE: (13) and FDODE:

(21) have coefficient matrices that are functions of the solution of the NLSE: (1). We compute the solutions of these equations in parallel, and at every z-step, the solution of NLSE: (1) is used to evaluate the coefficient matrices for COVODE: (13) and FDODE: (21).

The initial (launch) condition for NLSE: (1) is determined by the deterministic (or useful) part of the input excitation to the system. The subsection titles below, where appropriate, characterize the deterministic initial launch condition that is being considered. For example, in Section 5.7 below, we set the deterministic initial condition for NLSE: (1) to be the combination (summation) of a number of carriers modulated with random pulse streams.

The initial (launch) conditions for COVODE: (13) and FDODE: (21) are determined by the stochastic (noise) excitation on the system. For all of the results we present in this section, the initial condition for COVODE: (13) and FDODE: (21) is set up in such a way that it models a stochastic perturbation which is a white and stationary Gaussian noise (as a function of t). There may also be additional forcing terms in COVODE: (13) and FDODE: (21) which are localized in z, as described at the end of Section 3.2. These localized stochastic perturbations model noise added by discrete/lumped amplifiers to the system at certain sites along the propagation direction. Even though we have not considered distributed forcing terms in z for COVODE: (13) and FDODE: (21) (e.g., for modeling the noise added by distributed amplifiers), our formulations and computational techniques are general enough to handle such distributed stochastic perturbations, as explained in Section 3.2.

We have verified the accuracy and correctness of our numerical results by comparing them to analytical results for cases where such results are available. Moreover, the accuracy and consistency of our numerical results were also verified by comparing the stochastic perturbation characterizations obtained using the covariance matrix based approach (based on solving COVODE: (13)) with the ones obtained using the frequency-decomposed approach (based on solving FDODE: (21)). Comparison of our computational techniques with the Monte Carlo simulation based approaches, and comparisons with experimental (actual measurements on physical systems) results are part of the future work. The convergence behavior of the numerical methods presented in the paper is typical of spectral discretization for the time variable t, and of linear multistep methods for discretization in z.

We now present practical results obtained by an application of the formulations and the computational techniques developed in the paper to the investigation of signal–noise mixing due to the optical fiber nonlinearities in fiber-optic telecommunication systems. For a better appreciation of the results to be presented, and for definitions and terminology, please refer to Section 2.

5.1. System model

For the noise analysis examples we are going to present in this section, we use the model of an optical fiber communication link like the one shown in Fig. 1. The frequency separation between channels (difference between the center frequencies of the modulated carriers) was set to 25 GHz. The span length between amplifier sites was set to 80 km. In the link of Fig. 1, there is an OA before the first span of fiber. This OA sets the launch power for the channels, which was chosen as 10 mW/channel for all of the simulations that we will present. The WDM signal is launched into the link with the noise added by the first OA. The OAs along the link compensate for the loss of one span of fiber. They amplify the signal channels as well as the optical noise (which was added by the previous OAs along the link and "modified" by the fiber non-linearity). The parameters used for the single-mode fiber were: $\alpha = 0.25$ dB/km, $\beta_2 = -21.6$ ps^2/km, $\beta_3 = 0.128$ ps^3/km, $\gamma = 1.2$ W^{-1} km^{-1}. Thus, the loss of a fiber span with a length of 80 km is 20 dB. Hence, the OAs in the link have a power gain of 20 dB. The noise added by the OAs is modeled as a complex (with uncorrelated in-phase and quadrature components), white (constant spectral density) and stationary (constant power, i.e., variance, as a function of time) process. The

channel-combining and channel-selection bandpass filters in the WDM multiplexer [12] and WDM demultiplexer [13] were assumed to be ideal brick-wall filters.

For all of the examples we will present, number of Fourier modes for spectral time discretization N_f was set to 256, and 16 bits that repeat periodically were used in random pulse streams. The number of z-steps N_z depends on the truncation error tolerances and the frequency content of the signals being simulated. For signals with rich content in higher frequencies, smaller z-steps are required. For the simulations we performed, N_z ranged in 400–4000 for an 80 km length of fiber.

5.2. Fiber without non-linearity

If the fiber has no non-linearity, the noise analysis becomes trivial, because no signal–noise mixing occurs. The dispersion in the fiber still causes (linear) distortion to the signal channels. However, the second-order stochastic properties, i.e., the spectral density, of optical noise is *not* affected, because dispersion is equivalent to an all-pass filter with phase distortion. When a stochastic process passes through such a filter, its spectral properties remain unchanged. Thus, without non-linearity, the optical noise at the end of link, impinging on the receiver, is still stationary and white. The contribution from each OA to the total accumulated optical noise at the end of the link is the same, because the OAs compensate for the loss of one span of fiber. The optical noise from different OAs is assumed to be uncorrelated with each other.

5.3. Fiber without dispersion, and a single unmodulated carrier

The noise analysis for this very special case can be performed analytically, as was done by Gordon and Molleanuer [15]. In this case, optical noise (quadrature component with respect to the carrier) experiences (uncolored) amplification but stays white, and also stationary (assuming that the complex envelope in NLSE is centered at the single unmodulated carrier). We compared the numerical results we obtained with our noise simulator with the analytical results [14] in [15], and as expected, the agreement is exact.

5.4. Stationary vs non-stationary, white vs colored noise

Stationary noise is characterized by a time-domain covariance matrix $\mathbf{K}_t$ which is Hermitian and Toeplitz. In the spectral domain, the covariance matrix is diagonal, indicating that there is no *spectral correlation*. The spectral domain covariance matrix for non-stationary noise is non-diagonal, and in the time-domain, it is not Toeplitz. For instance, the values on the main diagonal (i.e., the variance or noise power as a function of time) of the time-domain covariance matrix are not equal for non-stationary noise. From now on and in the figures that will follow, we will use $\mathbf{K}_f$ to indicate the spectral domain covariance matrix, and $\mathbf{K}_t$ for the time-domain covariance matrix. Please recall that $\mathbf{K}_t$ is the covariance matrix for the time samples of optical noise, and both $\mathbf{K}_t$ and $\mathbf{K}_f$ are a function of z, the position along the fiber link. White noise is characterized by a diagonal $\mathbf{K}_t$ (indicating no correlation between the time samples of noise) and a Hermitian Toeplitz $\mathbf{K}_f$. Notice that this characterization is the *dual* of the characterization for stationary noise described above. Colored noise has a non-diagonal $\mathbf{K}_t$ and hence a non-Toeplitz $\mathbf{K}_f$. Note that white noise is not necessarily stationary. We can now deduce that white and stationary noise has a diagonal

[12] An ideal WDM multiplexer is a device which takes two (or more) signals (modulated carriers with different center frequencies) $m_1(t)\exp(\mathrm{j}\omega_{c1}t)$ and $m_2(t)\exp(\mathrm{j}\omega_{c2}t)$, and produces at its output the combined/composite signal $m_1(t)\exp(\mathrm{j}\omega_{c1}t)+m_2(t)\exp(\mathrm{j}\omega_{c2}t)$.

[13] An ideal WDM demultiplexer is a device which takes a composite signal $m_1(t)\exp(\mathrm{j}\omega_{c1}t)+m_2(t)\exp(\mathrm{j}\omega_{c2}t)$ composed of two (or more) signals (modulated carriers with different center frequencies) and produces $m_1(t)\exp(\mathrm{j}\omega_{c1}t)$ and $m_2(t)\exp(\mathrm{j}\omega_{c2}t)$ separately at its outputs.

[14] The results in [15] are approximate if the number of spans is not large, and they need to be modified to become exact for few spans.

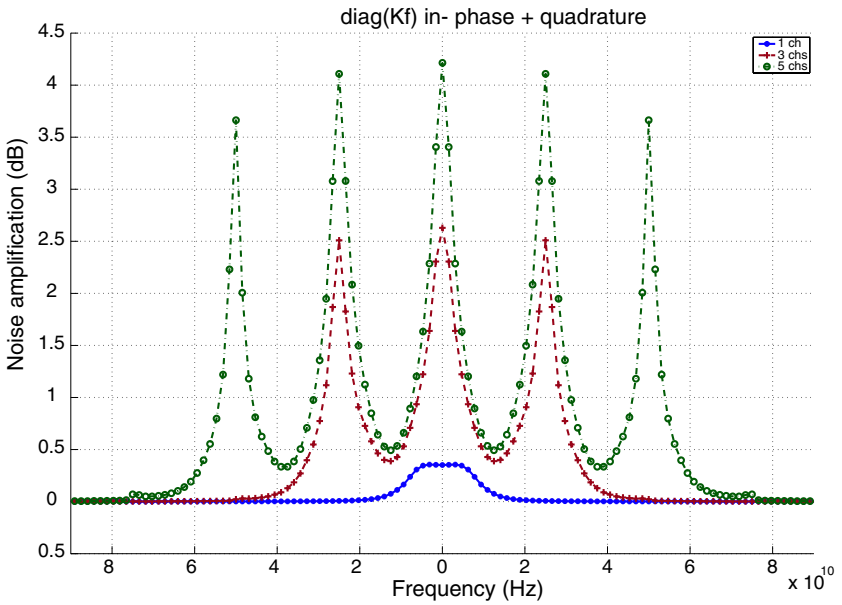

Fig. 3. Unmodulated carriers, diag($\mathbf{K}_f$): in-phase + quadrature.

$\mathbf{K}_f$ and diagonal $\mathbf{K}_t$ with constant entries on the diagonal. [15] The model that we use for the noise added by the OAs is white and stationary.

5.5. Comb of unmodulated carriers

We first present noise analysis results for the case of unmodulated carriers. We simulated a system like in Fig. 1 with 1, 3 and 5 WDM channels. Fig. 3 shows the main diagonal of $\mathbf{K}_f$ for the optical noise before the bandpass channel select filter (WDM demux) in the receiver. $\mathbf{K}_f$ in all of the figures we are going to present is normalized with the $\mathbf{K}_f$ one would obtain without any non-linearity in the fiber. Hence, the y-axis in all of $\mathbf{K}_f$ plots represents *noise amplification* (in dBs) due to signal–noise mixing. In Fig. 3, the total noise power, total for the in-phase and quadrature components, is shown. For the 5-channel case, the noise amplification at the carrier frequencies reaches $\sim$4 dB. It decreases rapidly as one moves away from the carrier frequencies. This decrease is due to dispersion in the fiber. Without dispersion, the noise amplification would have been uncolored, constant for all frequencies and equal to the value at $f = 0$. Hence, without dispersion, the effects of signal–noise mixing would have been *disastrous*. Moreover, as observed in Fig. 3, the increase in noise amplification (away from the carriers) from the 1-channel to the 3-channel case is more than the increase from the 3-channel case to the 5-channel one. This means that signal–noise mixing due to nearby channels is more severe than the noise–signal mixing due to channels further away. This is again due to dispersion. Without dispersion, the noise–signal mixing severity would be independent of the frequency separation between channels. The above is true only for noise amplification away from the carrier frequencies. The noise amplification at the carrier frequencies is not affected by dispersion and increases severely as the number of channels increase. In fact, the noise amplification at the carrier frequencies is directly proportional to the number of channels. However, the noise amplification away from the carrier

[15] Hermitian, Toeplitz and diagonal matrix = a scalar multiple of the identity matrix.

frequencies has a much milder dependence on the number of channels and does not increase much more as the number of channels is increased. With unmodulated carriers, the noise before the WDM demux is *non-stationary*, however it becomes stationary *after* the bandpass channel select filter.

5.6. Carriers modulated with a single pulse

We now present noise analysis results when the carriers are modulated with a single pulse. Upper plot in Fig. 4 shows the spectrum of the signal launched into the fiber, and also the signal spectrum at the end of the span. Bottom plot in Fig. 4 is the main diagonal of $\mathbf{K}_f$ before the channel select filter. For this case, the noise after the channel select filter is non-stationary, which can be observed from the non-diagonal $\mathbf{K}_f$ in Fig. 5.

5.7. Carriers modulated with random pulse stream

We will now compare the noise analysis results for unmodulated carriers and carriers modulated with a random pulse stream. Fig. 6 shows diag($\mathbf{K}_f$) for unmodulated and random pulse stream modulated carriers, both before the channel select filter. The average carrier power was kept equal for the two cases. We observe that, with modulation, the magnitude of noise amplification at the carrier frequency decreases. However, the noise amplification at frequencies away from, and in-between, the carriers increases. The total integrated noise power is approximately equal for these two cases. If we focus on the noise spectrum for the channel of interest centered at $f = 0$, there is more noise power in high frequencies in the modulated case compared with the unmodulated one. This, in time domain, corresponds to a *smaller* correlation width for

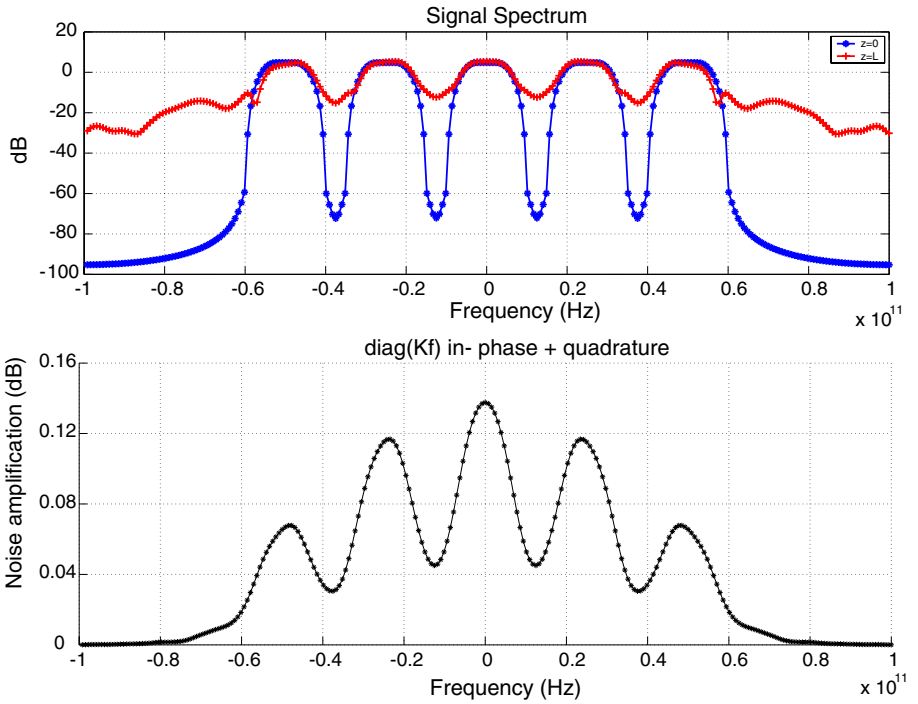

Fig. 4. Modulated carriers, single pulse, signal spectrum, diag($\mathbf{K}_f$).

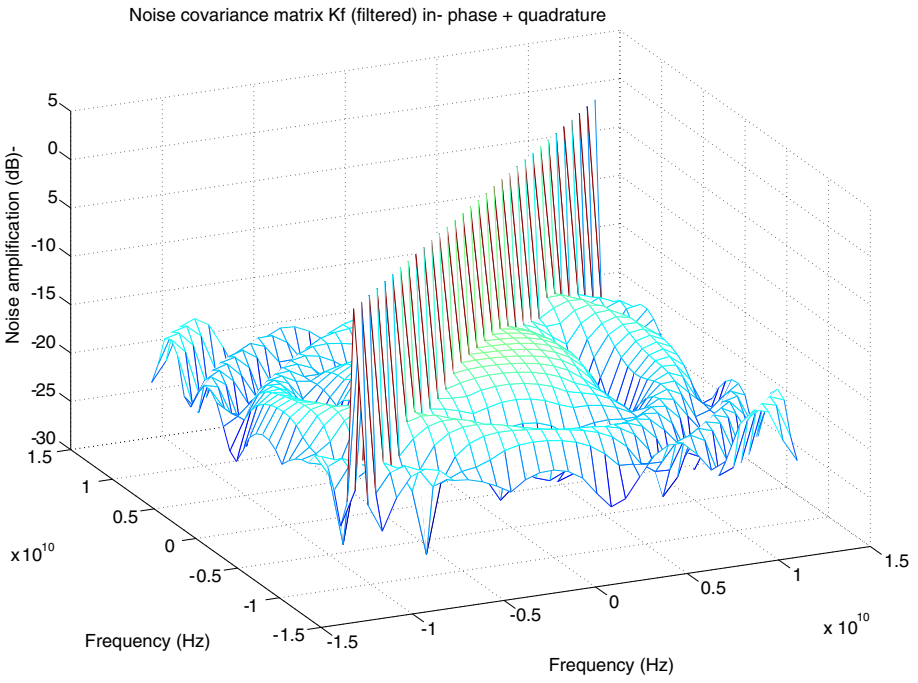

Fig. 5. Modulated carriers, single pulse, $\mathbf{K}_f$.

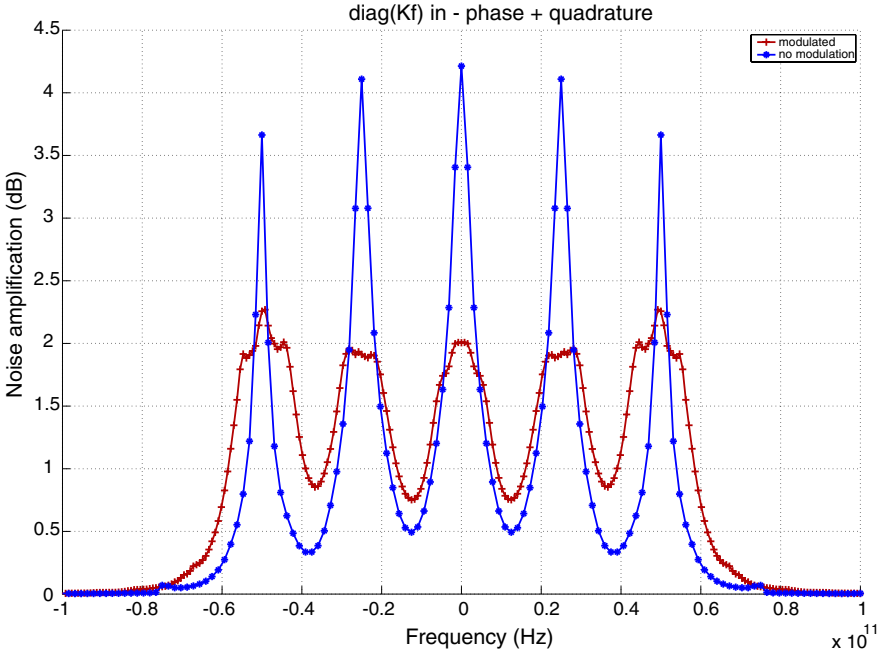

Fig. 6. Comparison between unmod. and mod. carriers: diag($\mathbf{K}_f$).

noise. In other words, if noise is sampled at the bit rate, then two consecutive samples will have a larger correlation in the unmodulated case compared with the modulated one.

Fig. 7 shows diag($\mathbf{K}_t$) for a carrier that was modulated with a random pulse stream, after the bandpass channel select filter. The noise in the unmodulated case is stationary after the channel select filter. However, it is non-stationary in the modulated case, with a time-varying noise variance, as observed in Fig. 7. In this case, the noise covariance matrix in the spectral domain is non-diagonal, as seen in Fig. 8.

5.8. System design implications and performance evaluation

The results we obtained above using the noise analysis methodology we developed and implemented have significant design implications, and can be used in system performance (BER) evaluations, which we briefly outline and summarize next.

Dispersion plays a significant role in the process of signal–noise mixing. The effects of noise–signal mixing would be *disastrous* without dispersion in the fiber.

With dispersion and non-linearity in the fiber, the optical noise experiences colored amplification due to signal–noise mixing, as seen in Fig. 6. Amplification is more severe around the carrier frequencies and it is proportional to the number of channels. Amplification away from the carrier frequencies is much smaller and has a very mild dependence on the number of channels. The optical noise sampled at the bit rate in the receiver has much larger power (compared with the case without signal–noise mixing) but the consecutive samples of noise becomes highly correlated due to low-frequency enhanced colored amplification. However, the correlation between consecutive samples is not as large as one would predict with unmodulated carriers. The modulation of the carriers results in a relatively smaller amplification of low (around the carriers) frequency noise and a relatively larger amplification of high (around the midpoint between the carriers) frequency noise. The correlation between consecutive noise samples can be used to guide the selection of the modulation scheme in system design. For instance, modulation schemes which encode data *differentially*

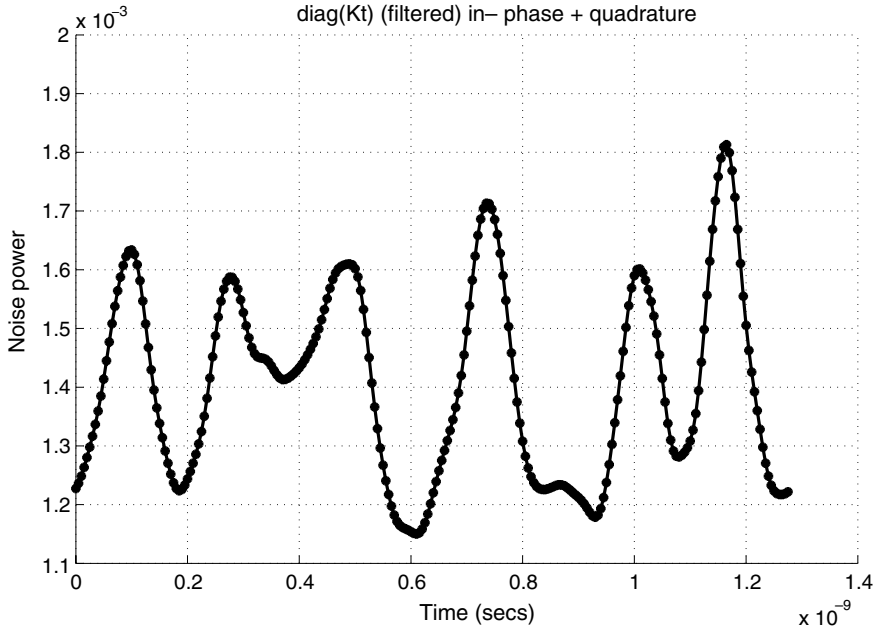

Fig. 7. Modulated carriers, random pulse stream, diag($\mathbf{K}_t$).

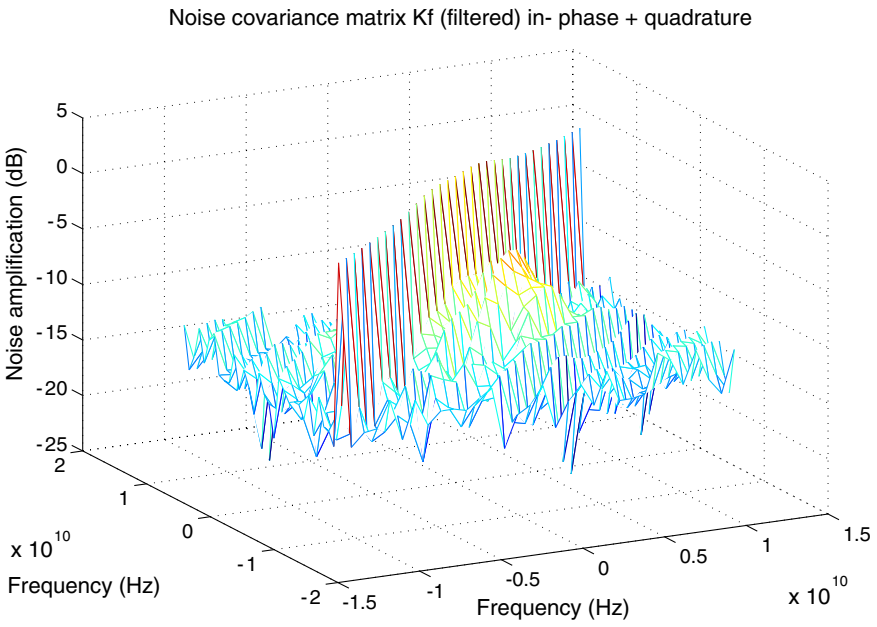

Fig. 8. Modulated carriers, random pulse stream, $\mathbf{K}_f$.

between two samples at the bit rate can make use of the correlation between the noise samples to improve BER performance in the presence of signal–noise mixing. Without signal–noise mixing, the optical noise stays white and the consecutive noise samples are uncorrelated.

The full stochastic characterization, including all correlation information, of optical noise samples at the receiver is available from the noise covariance matrices that our analysis techniques produce. This information can be used in BER performance evaluation.

6. Conclusions and future work

We have presented novel, non-Monte Carlo formulations and computational methods for the stochastic characterization of the solution of the stochastic non-linear Schrödinger equation. Our techniques are aimed at directly producing the ensemble-averaged probabilistic characterization desired for the solution of the stochastic non-linear Schrödinger equation, in a non-Monte Carlo manner without having to compute many realizations needed for ensemble-averaging. We are mainly motivated by the predominant role of the stochastic non-linear Schrödinger equation as a modeling tool in the design of optically amplified long distance fiber telecommunication systems. However, the usefulness of the work presented in the paper is by no means restricted to the analysis of optical fiber communication systems, and we plan to investigate other applications for our work in the analysis of other stochastic wave propagation phenomena, and also in the general setting of computational techniques for stochastic partial differential equations.

More efficient numerical methods and other high-order stiff z-stepping strategies for SNLSE, COVODE and FDODE, a parallelized and/or reduced-order-modeling based implementation of the frequency-decomposed formulation described in Section 3.3, investigation of efficient special-structure-exploiting representations for the noise covariance matrices are all part of the future work.

We plan to compare our computational techniques with the Monte Carlo simulation based approaches, and compare our results with the experimental ones obtained by actual measurements on physical systems.

We plan to include the implementations of the numerical techniques described in the paper in an analysis and design tool for optical fiber communication links to enable their use in the design of signal–noise mixing immune modulation schemes and for accurate and efficient system BER estimation.

Acknowledgements

The author thanks Professor Jacob White and his group at MIT for hosting him during Summer 2002. The author also likes to acknowledge the invaluable contribution of the anonymous reviewers whose comments and suggestions helped make the presentation of the contributions in the paper clearer and much more accessible to a general audience.

References

[1] C. Penland, A stochastic approach to nonlinear dynamics: a review, Am. Meteorol. Soc.
[2] G.P. Agrawal, Fiber-Optic Communication Systems, Wiley, New York, 2002.
[3] A. Demir, A. Sangiovanni-Vincentelli, Analysis and Simulation of Noise in Nonlinear Electronic Circuits and Systems, Kluwer Academic Publishers, Dordrecht, 1998.
[4] S. Habib, H. Kandrup, Nonlinear noise in cosmology, Phys. Rev. D 46 (1992) 5303.
[5] D. Lamberton, B. Lapeyre, Introduction to Stochastic Calculus Applied to Finance, Chapman & Hall, London, 1996.
[6] L. Arnold, Stochastic Differential Equations: Theory and Applications, Wiley, New York, 1974.
[7] V. Pugachev, I. Sinitsyn, Stochastic Differential Systems: Analysis and Filtering, Wiley, Chichester, Sussex, New York, 1987.
[8] C. Gardiner, Handbook of Stochastic Methods for Physics, Chemistry and the Natural Sciences, Springer, Berlin, 1983.
[9] J. Walsh, An introduction to stochastic partial differential equations, Lecture Notes in Mathematics, vol. 1180.
[10] P. Kloeden, E. Platen, Numerical Solution of Stochastic Differential Equations, Springer, Berlin, New York, 1992.
[11] A. Demir, A. Mehrotra, J. Roychowdhury, Phase noise in oscillators: a unifying theory and numerical methods for characterisation, IEEE Trans. Circuits Syst. I 47 (5) (2000) 655.
[12] A. Demir, Phase noise and timing jitter in oscillators with colored noise sources, IEEE Trans. Circuits Syst. I 49 (12) (2002) 1782.
[13] L.N. Trefethen, Spectral Methods in MATLAB, SIAM, Philadelphia, 2000.
[14] B. Fornberg, T.A. Driscoll, A fast spectral algorithm for nonlinear wave equations with linear dispersion, J. Comput. Phys. (155) (1999) 456–467.
[15] J.P. Gordon, L.F. Mollenauer, Phase noise in photonic communication systems using linear amplifiers, Opt. Lett. 15 (23) (1990) 1351.
[16] K. Kikuchi, Enhancement of optical-amplifier noise by nonlinear refractyive index and group-velocity dispersion of optical fibers, IEEE Photon. Technol. Lett. 5 (2) (1993) 221.
[17] G. Bosco, A. Carena, V. Curri, R. Gaudino, P. Poggiolini, S. Benedetto, Parametric gain in multiwavelength systems: a new approach to noise enhancement analysis, IEEE Photon. Technol. Lett. 11 (9) (1999) 1135.
[18] G.P. Agrawal, Nonlinear Fiber Optics, Academic Press, New York, 1995.
[19] P. Feldmann, Circuit noise evaluation by padé approximation based model-reduction techniques, in: IEEE/ACM International Conference on Computer-Aided Design, 1997.
[20] J. Roychowdhury, Reduced-order modelling of time-varying systems, IEEE Trans. Circuits Syst. II 46 (10) (1999) 1273.
[21] A.K. Kassam, L.N. Trefethen, Fourth-order time-stepping for stiff pdes, SIAM J. Sci. Comp. URL web.comlab.ox.ac.uk/oucl/work/nick.trefethen (to appear).
[22] G. Bosco, A. Carena, V. Curri, R. Gaudino, P. Poggiolini, S. Benedetto, Supression of spurious tones induced by the split-step method in fiber systems simulation, IEEE Photon. Technol. Lett. 12 (5) (2000) 489.
[23] E. Hairer, S.P. Norsett, G. Wanner, Solving Ordinary Differential Equations I: Nonstiff Problems, second ed., Springer, Berlin, Heidelberg, 1993.
[24] A. Hodel, S. Hung, Solution and applications of the lyapunov equation for control systems, IEEE Trans. Ind. Electron. 39 (3) (1992) 194.
[25] R. Bartels, G. Stewart, Solution of the equation $ax + xb = c$, Commun. ACM 15 (1972) 820–826.
[26] R.W. Freund, Model reduction methods based on Krylov subspaces, Acta Numerica 12 (2003) 267.